CHAPTER III - CONSTITUTIVE MODELS AND PARAMETERS STUDY

As shown in Chapter II, the constitutive modelling of concrete cracking phenomena has undergone tremendous development. Many constitutive models have been proposed in the past for analyzing concrete fracture, mainly for small-scale concrete structures such as single- or double-notched beams of mode I or mixed-mode fracturing.

Concrete dams are normally huge in size and are subjected to both normal and shear loadings, which results in a complex state of stress within the structures. As stated in Chapter II, the non-orthogonal crack model proposed by de Borst & Nauta (1985) is an ideal model to form the basis for the further development of models to simulate the cracking process in concrete dams under both normal and shear loadings. The constitutive relationships adopted in this research for the different deformation phases, such as the stages before and during softening, are outlined in the sections below.

In this research a smeared constitutive model has been established which has the advantages of preserving the topology of the finite element (FE) mesh and of easy determination of the crack orientation by aligning the crack perpendicular to the direction of principal stress during analysis. This model can be used to analyze the entire process of concrete cracking, including

- Pre-softening: Structural behaviour before a crack is initiated
- During softening: Structural behaviour during crack formation
- Structural behaviour for unloading/reloading and closing/reopening of cracks.

3.1 Pre-softening constitutive relationship

In this study, linear elastic behaviour in tension before the onset of a tensile fracture is assumed. For compression, linear elasticity is also assumed due to the fact that the research is focused on the local strain-softening behaviour of tensile fractured concrete and because the structures involved in this study, such as concrete gravity dams, are governed by cracking, not crushing. As a consequence, some non-elastic softening close to the peak

stress before a crack is initiated will be ignored by the above assumption. If required, a non-linear, plastic stress-strain law could be included later.

The incremental stress – incremental strain relationship is expressed as follows.

$$\Delta\sigma = D^{co}\,\Delta\varepsilon \tag{3.1}$$

- For 3-D FE analysis, equation (3.1) can be expressed as follows:

$$\begin{Bmatrix} \Delta\sigma_x \\ \Delta\sigma_y \\ \Delta\sigma_z \\ \Delta\sigma_{xy} \\ \Delta\sigma_{yz} \\ \Delta\sigma_{zx} \end{Bmatrix} = \frac{E}{(1+\nu)(1-2\nu)} \begin{bmatrix} 1-\nu & \nu & \nu & 0 & 0 & 0 \\ \nu & 1-\nu & \nu & 0 & 0 & 0 \\ \nu & \nu & 1-\nu & 0 & 0 & 0 \\ 0 & 0 & 0 & \frac{1-2\nu}{2} & 0 & 0 \\ 0 & 0 & 0 & 0 & \frac{1-2\nu}{2} & 0 \\ 0 & 0 & 0 & 0 & 0 & \frac{1-2\nu}{2} \end{bmatrix} \begin{Bmatrix} \Delta\varepsilon_x \\ \Delta\varepsilon_y \\ \Delta\varepsilon_z \\ \Delta\gamma_{xy} \\ \Delta\gamma_{yz} \\ \Delta\gamma_{zx} \end{Bmatrix} \tag{3.2}$$

Where

E	Young's modulus
ν	Poisson's ratio
x, y, z	Global Cartesian coordinates

- For plane stress analysis, the above equation (3.1) can be expressed as follows:

$$\begin{Bmatrix} \Delta\sigma_x \\ \Delta\sigma_y \\ \Delta\sigma_{xy} \end{Bmatrix} = \begin{bmatrix} \frac{E}{1-\nu^2} & \frac{\nu E}{1-\nu^2} & 0 \\ \frac{\nu E}{1-\nu^2} & \frac{E}{1-\nu^2} & 0 \\ 0 & 0 & G \end{bmatrix} \begin{Bmatrix} \Delta\varepsilon_x \\ \Delta\varepsilon_y \\ \Delta\gamma_{xy} \end{Bmatrix} \tag{3.3}$$

Where

G shear modulus, $G = \dfrac{E}{2(1+\nu)}$

- For plane strain analysis, the above equation (3.1) can be expressed as follows:

$$\begin{Bmatrix} \Delta\sigma_x \\ \Delta\sigma_y \\ \Delta\sigma_z \\ \Delta\sigma_{xy} \end{Bmatrix} = \frac{E}{(1+\nu)(1-2\nu)} \begin{bmatrix} 1-\nu & \nu & 0 & 0 \\ \nu & 1-\nu & 0 & 0 \\ \nu & \nu & 0 & 0 \\ 0 & 0 & 0 & \frac{1-2\nu}{2} \end{bmatrix} \begin{Bmatrix} \Delta\varepsilon_x \\ \Delta\varepsilon_y \\ \Delta\varepsilon_z = 0 \\ \Delta\gamma_{xy} \end{Bmatrix} \tag{3.4}$$

3.2 Crack onset criterion and crack direction

The crack onset criterion in this research is defined by assuming that the concrete will crack when the maximum tensile principal stress σ_1 exceeds the concrete tensile strength f_t at a Gauss point. The crack direction is then perpendicular to the direction of the maximum principal stress (see Figure 3.1).

This is a simple and effective conventional criterion which will ignore the effects of the second and third principal stresses under multi-axial loading conditions. For a 2-D application, the criterion is shown in straight lines in Figure 3.2. A more accurate crack initiation criterion (red curve in the Figure 3.2) depends on the second principal stress of the perpendicular direction, such as the criterion based on tensile strain energy density proposed by Bhattacharjee & Leger (1993).

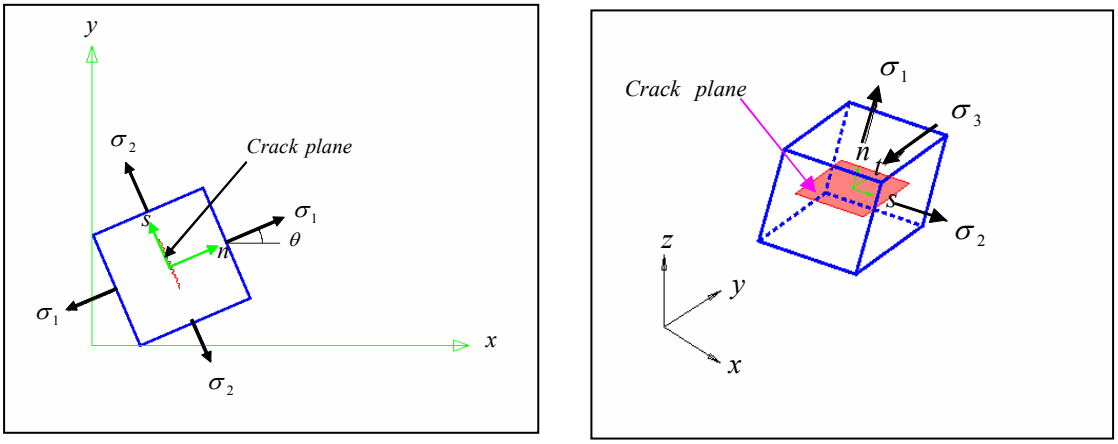

Figure 3.1 - Crack direction and local axis system for 2-D and 3-D applications

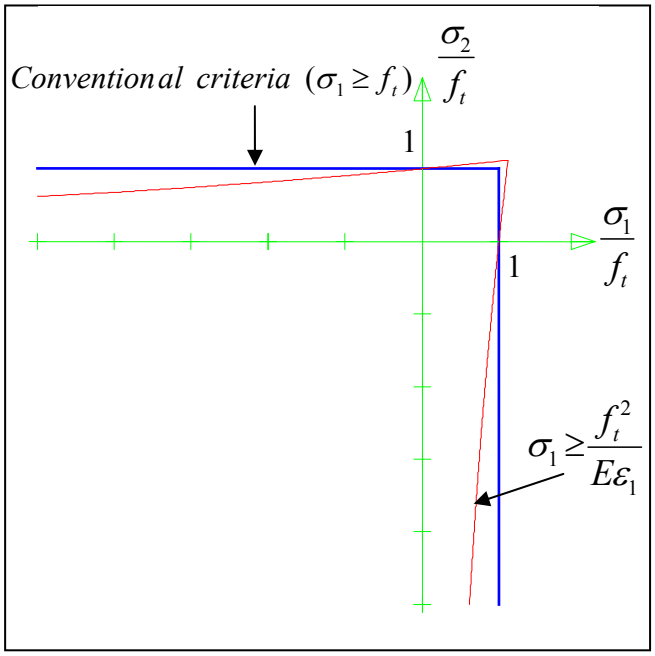

Figure 3.2 - Crack initiation criteria for a 2-D application

3.3 Constitutive relationship during concrete cracking

The early orthogonal crack models limited the crack formation and directions. Following cracking at one point, a second crack can be only allowed to form in the perpendicular direction of the first crack and so on. In 3-D modelling, a third crack may only develop perpendicular to the first two cracks. To improve cracking behaviour, de Borst and Nauta (1985) developed a non-orthogonal crack model, which allows a subsequent crack at a point to develop at any angle to a prior crack. This approach is ideal for simulating the cracking process in concrete structures. One of the main features of the model is that it decomposes the total crack strain increment into a strain increment for the uncracked concrete between cracks $\Delta\varepsilon^{co}$ and a strain increment at the crack $\Delta\varepsilon^{cr}$ as follows:

$$\Delta\varepsilon = \Delta\varepsilon^{co} + \Delta\varepsilon^{cr} \tag{3.5}$$

The crack strain increment $\Delta\varepsilon^{cr}$ in equation (3.5) is further contributed to by all the individual cracks at a particular Gauss point:

$$\Delta\varepsilon^{cr} = \Delta\varepsilon_1^{cr} + \Delta\varepsilon_2^{cr} + \cdots \tag{3.6}$$

Where $\Delta\varepsilon_1^{cr}$ is the strain increment of a first (primary) crack; $\Delta\varepsilon_2^{cr}$ is the strain increment of a secondary crack, and so on.

The strain increment of individual crack (i), $\Delta\varepsilon_i^{cr}$, in the global x, y and z coordinates can be obtained by transforming the local crack strain increment Δe_i^{cr} as follows:

$$\Delta\varepsilon_i^{cr} = N_i \Delta e_i^{cr} \tag{3.7}$$

$$\Delta e_i^{cr} = \begin{Bmatrix} \Delta e_{nn}^{cr} \\ \Delta\gamma_{ns}^{cr} \\ \Delta\gamma_{nt}^{cr} \end{Bmatrix}_i \tag{3.8}$$

The local coordinate system (n, s, t) is crack-aligned as shown in Figure 3.3, where n refers to the direction normal to a crack and s, t refer to the directions tangential to a crack.

In equation (3.8), Δe_{nn}^{cr} is the mode I local crack normal strain increment and $\Delta\gamma_{ns}^{cr}$, $\Delta\gamma_{nt}^{cr}$ are the mode II and III local crack shear strain increments respectively. N_i is a transformation matrix between the global and local coordinates at the crack (i).

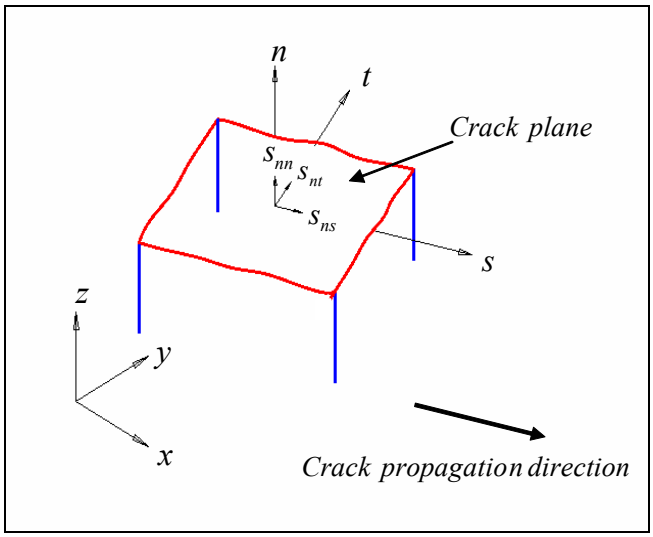

Figure 3.3 - Coordinate system and traction vectors across a crack for 3-D application

For a 3-D configuration, N_i has the following format:

$$N_i = \begin{bmatrix} l_1^2 & l_1 l_2 & l_3 l_1 \\ m_1^2 & m_1 m_2 & m_3 m_1 \\ n_1^2 & n_1 n_2 & n_3 n_1 \\ 2l_1 m_1 & l_1 m_2 + l_2 m_1 & l_3 m_1 + l_1 m_3 \\ 2m_1 n_1 & m_1 n_2 + m_2 n_1 & m_3 n_1 + m_1 n_3 \\ 2n_1 l_1 & n_1 l_2 + n_2 l_1 & n_3 l_1 + n_1 l_3 \end{bmatrix}_i \tag{3.9}$$

Where l_1, l_2, l_3, m_1, m_2, m_3, n_1, n_2, n_3 are the direction cosines of the axes defined in Tables 3.1 and 3.2 (refer to Figures 3.1 and 3.3):

TABLE 3.1 - Direction cosines of local axes in global axis

	x	y	z	Global coordinate
n	l_1	m_1	n_1	
s	l_2	m_2	n_2	
t	l_3	m_3	n_3	
Local coordinate				

For a 2-D application (plane stress or plane strain), Table 3.1 becomes the following Table 3.2.

TABLE 3.2 - Direction cosines of local axes in global axis (2-D)

Local coordinate	x	y	z	Global coordinate
n	$l_1 = cos\theta$	$m_1 = sin\theta$	$n_1 = 0$	
s	$l_2 = -sin\theta$	$m_2 = cos\theta$	$n_2 = 0$	
t	$l_3 = 0$	$m_3 = 0$	$n_3 = 1$	

Where θ is the angle between the normal of a crack and the global x-axis shown in Figure 3.1.

For equation (3.7), it is convenient to assemble the individual crack vectors and matrices into a general form as follows.

$$\Delta\varepsilon^{cr} = N\,\Delta e^{cr} \tag{3.10}$$

Where $N = [N_1\ N_2 \cdots]$ is a transformation matrix which combines all the individual crack transformation matrices, and $\Delta e^{cr} = [\Delta e_1^{cr}\ \Delta e_2^{cr} \cdots]^T$ is the local crack strain increment which is composed of the contributions of multiple cracks.

The local stress increment ΔS^{cr} can be derived by transforming the global stress increment $\Delta\sigma$ as follows:

$$\Delta S^{cr} = N^T\,\Delta\sigma \tag{3.11}$$

Where $\Delta S^{cr} = [\Delta S_1^{cr}\ \Delta S_2^{cr} \cdots]^T$ is composed of the contributions of multiple cracks.

For an individual crack (*i*), the local crack stress increment vector ΔS_i^{cr} is defined as:

$$\Delta S_i^{cr} = \begin{Bmatrix} \Delta S_{nn}^{cr} \\ \Delta S_{ns}^{cr} \\ \Delta S_{nt}^{cr} \end{Bmatrix}_i \tag{3.12}$$

Where ΔS_{nn}^{cr} is the mode I normal stress increment and $\Delta S_{ns}^{cr}, \Delta S_{nt}^{cr}$ are the mode II and III shear stress increments respectively.

The constitutive relationships of the concrete between the cracks and the local cracks are as follows:

$$\Delta\sigma = D^{co}\,\Delta\varepsilon^{co} \tag{3.13}$$

$$\Delta S^{cr} = D^{cr}\,\Delta e^{cr} \tag{3.14}$$

Where

D^{co} is the constitutive matrix of the 'intact' concrete between the cracks as follows:

$$D^{co} = \frac{E}{(1+\nu)(1-2\nu)} \begin{bmatrix} 1-\nu & \nu & \nu & 0 & 0 & 0 \\ \nu & 1-\nu & \nu & 0 & 0 & 0 \\ \nu & \nu & 1-\nu & 0 & 0 & 0 \\ 0 & 0 & 0 & \frac{1-2\nu}{2} & 0 & 0 \\ 0 & 0 & 0 & 0 & \frac{1-2\nu}{2} & 0 \\ 0 & 0 & 0 & 0 & 0 & \frac{1-2\nu}{2} \end{bmatrix} \tag{3.15}$$

and

D^{cr} is the constitutive matrix of the local cracks as follows:

$$D^{cr} = \begin{bmatrix} D_1^{cr} & 0 & \cdots \\ 0 & D_2^{cr} & \cdots \\ \cdots & \cdots & \cdots \end{bmatrix} \tag{3.16}$$

Where the size (columns and rows) of D^{cr} depends on the number of cracks at the Gauss point. Zero off-diagonal terms implies that the coupling effects between different cracks are ignored.

For a crack (i): $D_i^{cr} = \begin{bmatrix} D_i^I & 0 & 0 \\ 0 & D_i^{II} & 0 \\ 0 & 0 & D_i^{III} \end{bmatrix}$ in which D_i^I is the mode I stiffness modulus, $D_i^{II} = \frac{\beta}{1-\beta} G$ is the mode II shear stiffness modulus and D_i^{III} is the mode III stiffness modulus. β is the shear retention factor to be defined in Section 3.5. $G = \frac{E}{2(1+\nu)}$ is the elastic shear modulus. Again, no coupling is considered between the shear and normal strains on the crack plane.

From equations (3.11), (3.13), (3.5) and (3.10), we have:

$$\Delta S^{cr} = N^T \Delta\sigma = N^T D^{co} \Delta\varepsilon^{co} = N^T D^{co} (\Delta\varepsilon - N\Delta e^{cr}) \tag{3.17}$$

From equations (3.17) and (3.14), we have:

$$D^{cr} \Delta e^{cr} = N^T D^{co} (\Delta\varepsilon - N\Delta e^{cr}) \tag{3.18}$$

From equation (3.18), we have:

$$(D^{cr} + N^T D^{co} N)\Delta e^{cr} = N^T D^{co} \Delta\varepsilon \tag{3.19}$$

From equation (3.19), we have:

$$\Delta e^{cr} = \left[D^{cr} + N^T D^{co} N\right]^{-1} N^T D^{co} \Delta\varepsilon \tag{3.20}$$

From equations (3.20) and (3.13), (3.5) and (3.10), we have:

$$\Delta\sigma = D^{co}\left\{\Delta\varepsilon - N\left[D^{cr} + N^T D^{co} N\right]^{-1} N^T D^{co} \Delta\varepsilon\right\} \tag{3.21}$$

The overall relationship between global stress and strain is obtained from the above equation (3.21):

$$\Delta\sigma = \left\{D^{co} - D^{co} N\left[D^{cr} + N^T D^{co} N\right]^{-1} N^T D^{co}\right\}\Delta\varepsilon \tag{3.22}$$

3.3.1 Plane stress application used in this research

For the plane stress analysis in equation (3.22), we have:

$$D^{co} = \begin{bmatrix} \dfrac{E}{1-\nu^2} & \dfrac{\nu E}{1-\nu^2} & 0 \\ \dfrac{\nu E}{1-\nu^2} & \dfrac{E}{1-\nu^2} & 0 \\ 0 & 0 & \dfrac{E}{2(1+\nu)} \end{bmatrix} \tag{3.23}$$

$$D^{cr} = \begin{bmatrix} D_1^{cr} & 0 & \cdots \\ 0 & D_2^{cr} & \cdots \\ \cdots & \cdots & \cdots \end{bmatrix} \tag{3.24}$$

$$\Delta S_i^{cr} = D_i^{cr}\,\Delta e_i^{cr} \quad \Longrightarrow \quad \begin{Bmatrix} \Delta S_{nn}^{cr} \\ \Delta S_{ns}^{cr} \end{Bmatrix}_i = \begin{bmatrix} D_i^{I} & 0 \\ 0 & D_i^{II} \end{bmatrix} \begin{Bmatrix} \Delta e_{nn}^{cr} \\ \Delta \gamma_{ns}^{cr} \end{Bmatrix}_i \tag{3.25}$$

Where D_i^I is the mode I stiffness, which will be discussed in the next section, Section 3.4.

$D_i^{II} = \dfrac{\beta}{1-\beta} G$ is the mode II stiffness, which will be discussed in the Section 3.5.

$N = \left[N_1 \, N_2 \cdots \right]$ is the overall transformation matrix composed of all the transformation matrices (equation 3.26) of each individual crack at a point.

The transformation matrix of an individual crack (i) reduces to a 3 x 2 matrix from equation (3.9) as follows:

$$N_i = \begin{bmatrix} l_1^2 & l_1 l_2 \\ m_1^2 & m_1 m_2 \\ 2l_1 m_1 & l_1 m_2 + l_2 m_1 \end{bmatrix}_i = \begin{bmatrix} \cos^2\theta_i & -\cos\theta_i \sin\theta_i \\ \sin^2\theta_i & \cos\theta_i \sin\theta_i \\ 2\cos\theta_i \sin\theta_i & \cos^2\theta_i - \sin^2\theta_i \end{bmatrix} \tag{3.26}$$

Where θ_i is the angle between the normal of a crack (i) and the global x-axis shown in Figure 3.1.

3.3.2 Plane strain application used in this research

For the plane strain analysis in equation (3.22), we have:

$$D^{co} = \frac{E}{(1+\nu)(1-2\nu)} \begin{bmatrix} 1-\nu & \nu & 0 & 0 \\ \nu & 1-\nu & 0 & 0 \\ \nu & \nu & 0 & 0 \\ 0 & 0 & 0 & \frac{1-2\nu}{2} \end{bmatrix} \tag{3.27}$$

$$D^{cr} = \begin{bmatrix} D_1^{cr} & 0 & \cdots \\ 0 & D_2^{cr} & \cdots \\ \cdots & \cdots & \cdots \end{bmatrix} \tag{3.28}$$

$$\Delta S_i^{cr} = D_i^{cr} \, \Delta e_i^{cr} \quad \Longrightarrow \quad \begin{Bmatrix} \Delta S_{nn}^{cr} \\ \Delta S_{ns}^{cr} \end{Bmatrix}_i = \begin{bmatrix} D_i^{I} & 0 \\ 0 & D_i^{II} \end{bmatrix} \begin{Bmatrix} \Delta e_{nn}^{cr} \\ \Delta \gamma_{ns}^{cr} \end{Bmatrix}_i \tag{3.29}$$

Where D_i^I is the mode I stiffness, which will be discussed in the next section, Section 3.4.

$D_i^{II} = \dfrac{\beta}{1-\beta} G$ is the mode II stiffness, which will be discussed in Section 3.5.

Equation (3.28) is the same as equation (3.24), and equation (3.29) is the same as equation (3.25).

$N = \left[N_1 \, N_2 \cdots \right]$ is the transformation matrix composed of all the transformation matrices (equation 3.30) of each individual crack at a point.

The transformation matrix of an individual crack (i) reduces to a 4 x 2 matrix from equation (3.9) as follows:

$$N_i = \begin{bmatrix} l_1^2 & l_1 l_2 \\ m_1^2 & m_1 m_2 \\ n_1^2 & n_1 n_2 \\ 2l_1 m_1 & l_1 m_2 + l_2 m_1 \end{bmatrix}_i = \begin{bmatrix} \cos^2\theta_i & -\cos\theta_i \sin\theta_i \\ \sin^2\theta_i & \cos\theta_i \sin\theta_i \\ 0 & 0 \\ 2\cos\theta_i \sin\theta_i & \cos^2\theta_i - \sin^2\theta_i \end{bmatrix} \tag{3.30}$$

3.4 Mode I tensile softening

In equation (3.22), the constitutive matrix of the local crack at a Gauss point is composed of all the individual cracks at that point. For any one crack (i) at that point, the mode I stiffness of the crack, D_i^I, is dependent on the fracture energy G_f of the material, which is defined as the energy dissipation for a unit area of a mode I (tension) crack plane propagation, the shape of the tensile softening diagram, the direct tensile strength f_t and the crack blunt width h_c. The fracture energy G_f and the direct tensile strength f_t are taken as fixed material properties for a specific concrete. The crack blunt width h_c will be discussed later in Section 3.7. The shape of the crack softening diagram for mode I fracturing of concrete would significantly change the values of the mode I softening modulus and is still a much-debated matter. The mode I softening diagram could take

various forms. Linear, bilinear and non-linear curves have been adopted in past and current analyses of the cracking of concrete structures (refer to Figure 3.4).

Linear strain softening (see for example Figure 3.5) has been widely adopted in the fracture analysis of concrete structures, in particular for concrete dams. The mode I stiffness modulus of a local crack is defined as follows:

$$D_{i,l}^{I} = \frac{EE_s}{E - E_s} = -\frac{f_t^2 h_c}{2G_f} \tag{3.31}$$

Where E_s is the strain-softening modulus shown in Figure 3.5. In Figures 3.5 and 3.6, e_n is the normal strain of cracked concrete in a local coordinate system (sum of the normal strains of the concrete between cracks and of the cracks themselves). S_n^{cr} is the normal stress in the local crack. e_{nn}^{cr} is the normal strain in the local crack. e_n^f is the ultimate normal crack strain, after which tensile stress vanishes.

Various experimental studies have revealed that concrete actually fractures in a non-linear softening format, where an exponential softening curve best fits the experimental data as done by Cornelissen, Hordijk & Reinhardt (1986). However, since a non-linear softening curve is normally difficult to implement in the analysis, it is not considered justified at this stage for practising engineers to use this non-linear softening approach. A bilinear softening strategy is adopted in this research to approximate the real softening curve by adjusting the values of the two shape parameters α_1 and α_2 (refer to Figure 3.6), while maintaining simplicity of implementation.

For the purpose of this research, the following bilinear strain-softening equations were developed:

$$G_f = -\frac{h_c}{2}\left[\frac{(\alpha_1 f_t + f_t)(1-\alpha_1) f_t}{D_{i,bl}^{I}} + \frac{\alpha_1^2 f_t^2}{\alpha_2 D_{i,bl}^{I}}\right] = -\frac{f_t^2 h_c}{2}\left[\frac{\alpha_2 + (1-\alpha_2)\alpha_1^2}{\alpha_2 D_{i,bl}^{I}}\right] \tag{3.32}$$

$$D_{i,bl}^{I} = \frac{\alpha_2 + (1-\alpha_2)\alpha_1^2}{\alpha_2}\left(-\frac{f_t^2 h_c}{2G_f}\right) = \frac{\alpha_2 + (1-\alpha_2)\alpha_1^2}{\alpha_2} D_{i,l}^{I} \tag{3.33}$$

Where α_1 and α_2 are bilinear softening shape parameters. α_1 is defined as the portion of the tensile strength below which the strain softening becomes flattened (the mode I softening modulus uses the second slope line of softening). α_2 is defined as the ratio of the second softening modulus to the first softening modulus.

$D_{i,bl}^{I}$ is the first mode I softening modulus in the bilinear softening diagram (refer to Figure 3.6), which is controlled by the shape parameters of the softening diagram (α_1 and α_2), the fracture energy G_f, the direct tensile strength f_t and the crack blunt width of the finite elements h_c.

When $\alpha_1 = 0$, $D_{i,bl}^{I} = D_{i,l}^{I}$, the strain softening becomes linear

When $\alpha_2 = 1$, $D_{i,bl}^{I} = D_{i,l}^{I}$, the strain softening becomes linear.

Figure 3.7 shows how the shapes of the bilinear diagram are changed and their relationship with the linear mode I softening modulus $D_{i,l}^{I}$ if α_1 is fixed at 1/3 while α_2 is taken as 0.1, 0.2 and 0.3 respectively.

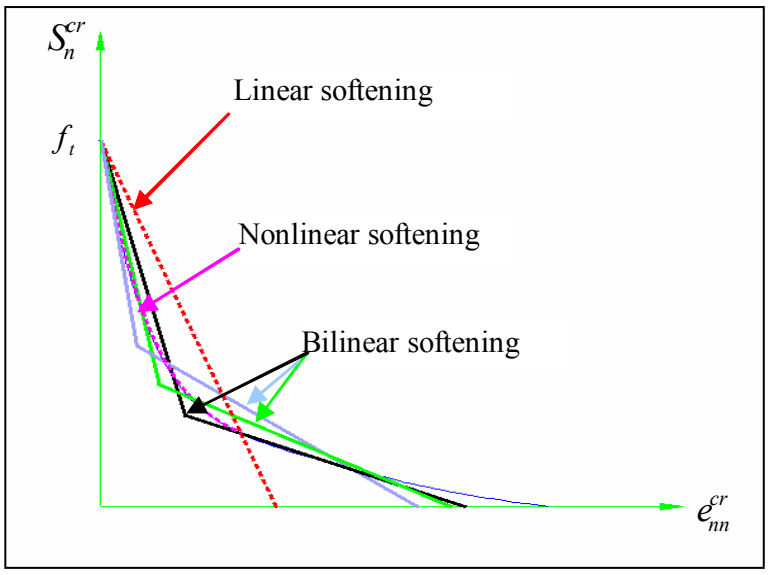

Figure 3.4 - Linear, bilinear and curved mode I strain-softening diagram of "crack"

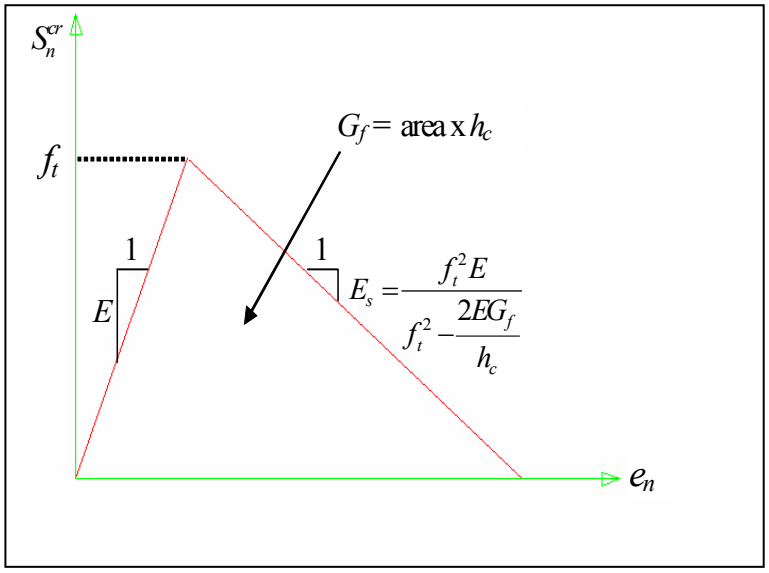

Figure 3.5 - Linear elastic – mode I strain-softening diagram of cracked concrete

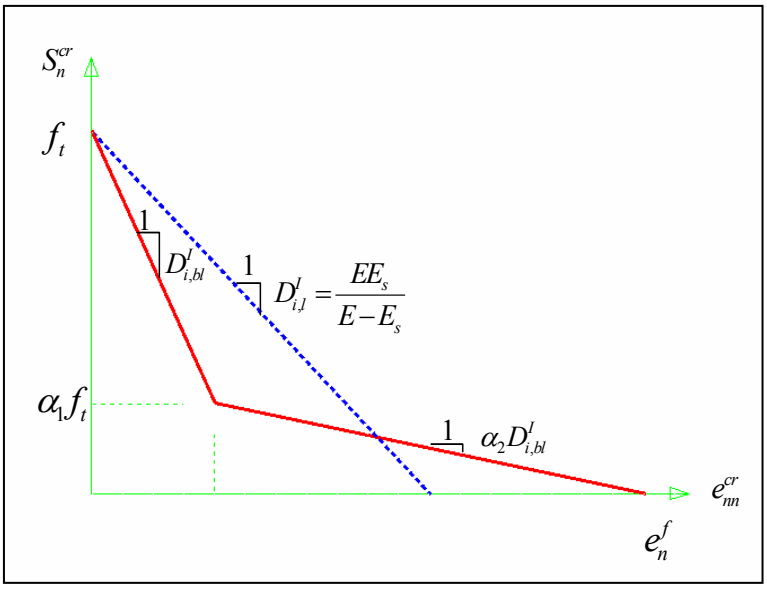

Figure 3.6 - Definition of bilinear mode I strain-softening diagram of “crack”

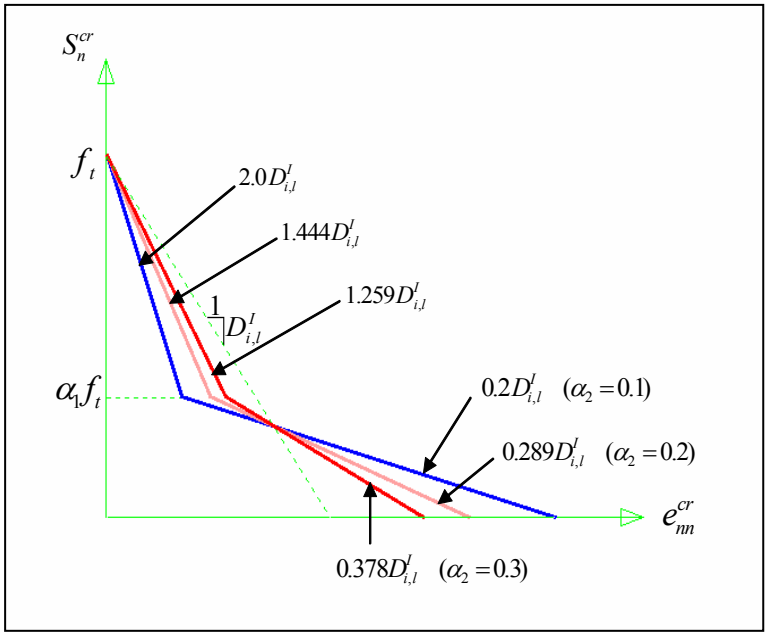

Figure 3.7 - Bilinear mode I strain-softening diagrams for α_1 = 1/3; α_2 = 0.1, 0.2 and 0.3 (local coordinate)

3.5 Mode II shear softening

Due to aggregate interlock in plain concrete, the shear modulus does not reduce to zero immediately after cracking. Therefore, shear stress can be developed on the plane of a crack at subsequent loading. In the past, a simple non-zero shear retention factor β was adopted to represent shear softening in modelling concrete cracking (Bhattacharjee & Leger 1993; Lotfi & Espandar 2004). However, this method ignores the shear dilation and the dependence of crack shear on the crack opening displacement. This also results in a constant cracking shear modulus that cannot take into account the fact that the shear strain varies with the normal crack strain, as observed in experimental studies. For this research, the shear stiffness of a crack is defined as a decreasing function of the crack normal strain in the following formula (equation 3.34), which is similar to that used by Rots & Blaauwendraad (1989), except for a maximum shear retention factor β_{max} defined here to limit the maximum shear allowed in a crack. The value of β_{max} usually varies from 0 to 0.5. A high shear retention value (β close to 0.5) could cause extensive cracking in certain applications, while zero retention (β = 0) could result in numerical instabilities (Lotfi & Espandar 2004).

$$\beta = \beta_{\max} (1 - \frac{e_{nn}^{cr}}{e_n^f})^p \tag{3.34}$$

Where e_{nn}^{cr} and e_n^f have been defined previously and p is a constant defining the shear-softening shape. As shown in Figure 3.8, if p=0, $\beta = \beta_{\max}$ (constant); if p=1, shear softening is in a descending linear format; if p=2, shear softening is in a descending non-linear format.

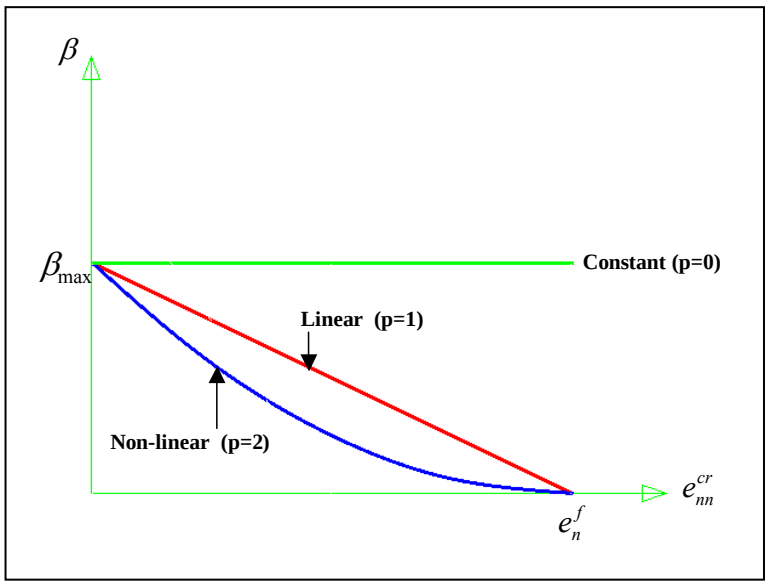

Figure 3.8 - Relationship between shear retention factor and "crack" strain (local coordinate)

3.6 Fixed/rotating, unloading/reloading and closing/reopening of cracks

As stated previously, the direction of cracking is generally aligned perpendicular to the principal stress direction and is fixed after the crack has been initiated in the fixed non-orthogonal crack model. Each fixed crack is "remembered" with its own direction and is kept unaltered for the rest of analysis. This permanent "memory" of crack directions increases the cost of computation.

After cracking, the shear stresses would cause the principal stress axes to rotate, which could increase the tensile principal stresses well above the concrete tensile strength. In this

research, a new crack is initiated whenever the angle between the normal to the crack plane of the last crack and the current principal stress direction exceeds a pre-defined threshold angle or whenever the inclined tensile principal stress σ_1 violates the crack onset criterion. The reason why the above new crack initiation criterion is adopted will now be explained.

If only the stress criterion applies (i.e. if the maximum tensile principal stress exceeds the material's tensile strength), then the total number of cracks cannot be limited. For example, if high shear stress remains in a crack, a new crack could be initiated with almost every loading increment, which would render the analysis inefficient. On the other hand, the threshold angle condition (i.e. when the angle between the principal stress and the last existing crack exceeds a threshold angle) does not control the maximum tensile stress. A tensile principal stress three times higher than the tensile strength could occur without violating the threshold angle condition (Rots & Blaauwendraad 1989). Only if these two conditions are combined can a reasonable new crack initiation criterion be established.

Depending on the magnitude of the pre-defined threshold angle, many cracks could occur at a Gauss point. For the purpose of limiting the computing memory required and making the multi-directional crack model more robust, a maximum of six cracks are allowed to form at a Gauss point. The effect of each additional crack on the results becomes progressively and significantly less as the number of cracks at a point increases.

Concrete structures are normally subjected to both tension and shear stress conditions. The mixed-mode fracturing behaviour leads to the rotation of the axes of principal stress after a crack is formed. Consequently, the fixed crack axes no longer represent the axes of principal stress. The fixed, multi-directional, non-orthogonal crack model adopted here is able partially to reduce the misalignment between the crack orientation and the principal direction.

Alternatively, a rotating approach can be used in which the normal axis to the crack plane is allowed to co-rotate with the principal stress axis. A rotating crack concept, in which the axes of a crack co-rotate with the orientation of the principal stress, has been proposed

in the past to eliminate the discrepancy between and the misalignment of the crack directions and principal directions.

Rots & Blaauwendraad (1989) proposed a rotating crack model by simply vanishing the threshold angle and making all previous cracks inactive, erasing them from memory. In this way, the crack orientation changes continuously to align with the direction of principal stress. The following three conditions were set for the rotating model by Rots & Blaauwendraad (1989):

- The orientation of subsequent cracks is only controlled by setting the threshold angle to zero.
- Only the current crack is allowed to remain active, by erasing all previous cracks at the Gauss point.
- The influence of previous cracks is accounted for and the mode II shear-softening modulus D^{II} in the following equation (3.36) is used to ensure coaxiality.

In order to enforce coaxiality between the principal stress and strain, the softening shear modulus for a 2-D analysis should be calculated as follows:

$$\beta G = \frac{\sigma_1 - \sigma_2}{2(\varepsilon_1 - \varepsilon_2)} \tag{3.35}$$

$$\frac{1}{\beta G} = \frac{1}{G} + \frac{1}{D^{II}} \quad \Rightarrow \quad D^{II} = \frac{\sigma_1 - \sigma_2}{2(\varepsilon_1 - \varepsilon_2)G - (\sigma_1 - \sigma_2)} \tag{3.36}$$

The proposed fixed, multi-directional, non-orthogonal crack model can be converted into a rotating model by applying the above-mentioned conditions for the rotating crack approach.

The post-fracturing behaviour forms an important part of the crack constitutive model. The unloading/reloading and closing/reopening strategy used is shown in Figures 3.9 and 3.10. A secant unloading approach is adopted in this study, which implies that the crack stress-strain relationship follows a path back to the origin upon a strain reduction. This

strategy is often used by researchers since it yields a closer approximation to the real unloading behaviour of concrete for application in smeared based crack models than the elastic unloading approach used in the past, in which the crack closes immediately during a strain reduction (Calayir & Karaton 2005; Rots 2002; Cervera *et al*. 1990).

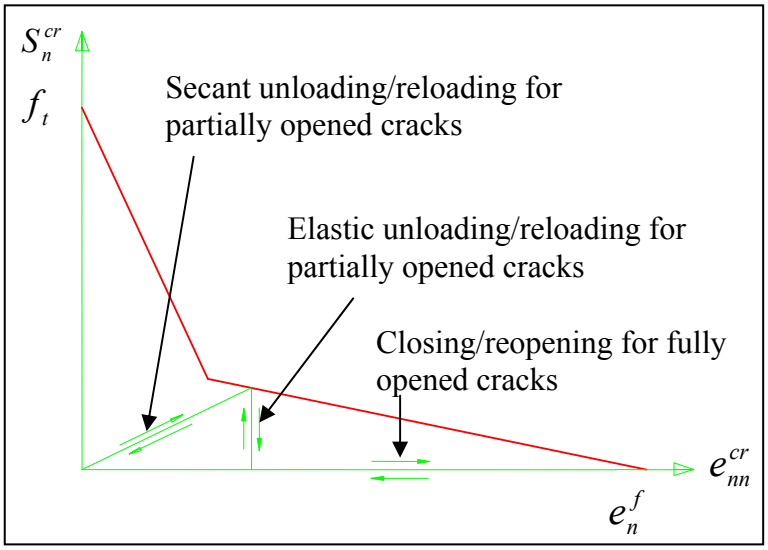

Figure 3.9 - Diagram of unloading/reloading and closing/reopening (in crack strain)

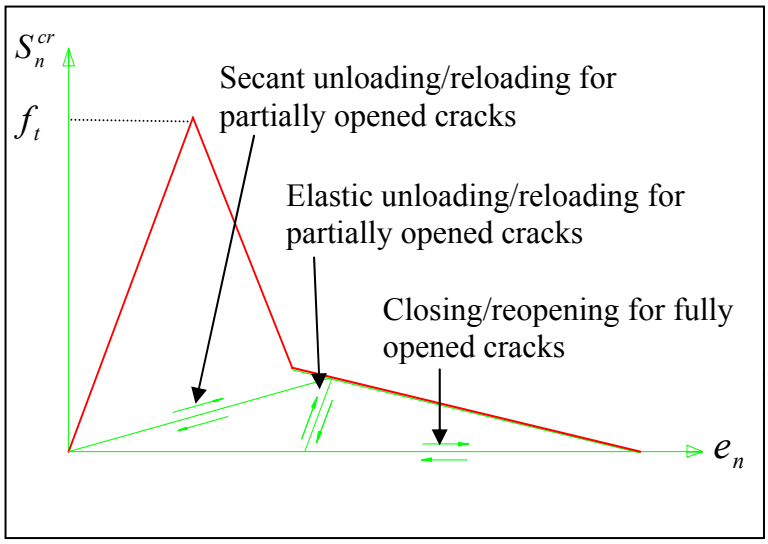

Figure 3.10 - Diagram of unloading/reloading and closing/reopening (in total strain)

3.7 Width of crack blunt front and mesh objectivity

In the smeared crack approach, a crack in an element is formed and propagated over an area related to the size of the element. The characteristic length of the crack band in smeared modelling must be defined in order to obtain mesh objectivity. The fracture process is assumed to occur in bands of micro-defects over a so-called *crack band width*. Gajer & Dux (1990) treated the width of the crack band as a material property, which should be three to ten times the maximum aggregate size.

Bhattacharjee & Leger (1992) distinguished between the characteristic length h_c in non-linear fracture mechanics models and the width of the crack band w_c in the crack band model (Bažant & Oh 1983). Unlike the crack band width w_c, the characteristic dimension h_c is a geometric property of the cracking element (refer to Figures 2.6 and 2.7 in Chapter II for illustrations of w_c and h_c).

The introduction of a characteristic length h_c into the determination of the mode I softening modulus is a step towards a non-local softening model for mesh objectivity.

The following definition of the crack characteristic length h_c has been proposed by researchers in the past:

- $h_c = \sqrt{Area\ of\ element}$; i.e. square root of the area of the cracking element for a 2-D application (Bhattacharjee & Leger 1992) or
- h_c = size of the cracking element, across the direction of crack propagation (Bhattacharjee & Leger 1992).
- h_c is taken as the side of an equivalent cube having the same volume as the tributary volume at the cracked point of a solid isoparametric element for a 3-D application (Lotfi & Espandar 2004).
- $h_c = \sqrt{2} \times size\ of\ the\ cracking\ element$ (Rots & Blaauwendraad 1989).

A more rigorous description of h_c, which is dependent on the mesh size, crack direction and spatial position, can be found in the paper by Oliver (1989).

In this research, the response quantities of elements were computed at each integration point of the elements. Thus, the size adjustment of the strain-softening modulus E_s (refer to Figure 3.5) and the fracture energy dissipation are determined on the basis of local response quantities. The crack characteristic length h_c is defined as the size of the element across the crack direction if the finite element mesh is oriented to be parallel to the crack band (Figure 3.11(a)). If a crack is propagating obliquely through an element, as shown in Figure 3.11(b), then h_c is defined as the square root of the element area.

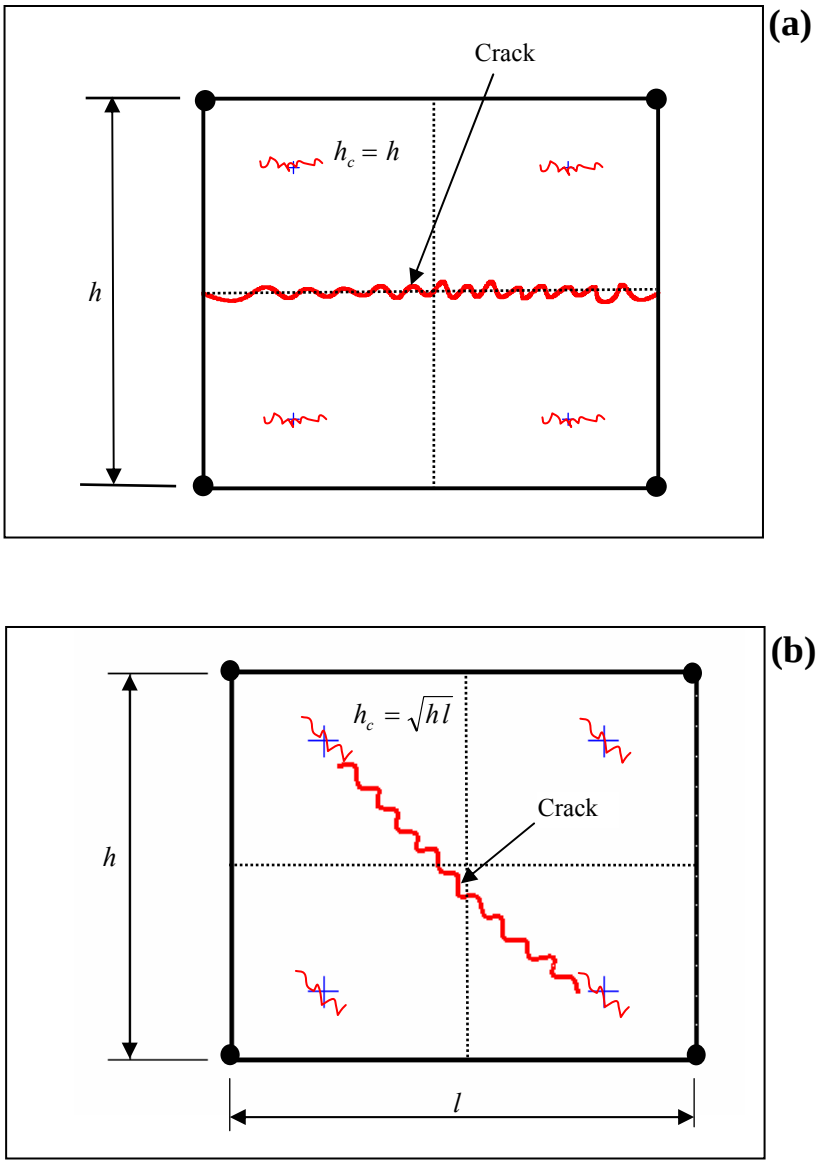

Figure 3.11 - Crack characteristic length h_c of a quadrilateral element (first order with full integration)

3.8 Element selection for crack analysis

The application of reduced integration is less reliable than the normal integration element. It could induce a spurious hour-glass mode, which could easily cause divergence of the iterative procedure. Dodds, Darwin, Smith & Leibengood (1982) investigated the hour-glassing problems and suggested that reduced integration elements should not be used. In this research, first-order elements with full integration have been selected for the analysis of concrete cracking, as used by many researchers in the past (Bhattacharjee & Leger 1993; Bhattacharjee & Leger 1994; Rots & Blaauwendraad 1989). Second-order elements can also be used for the proposed smeared crack model if needed.

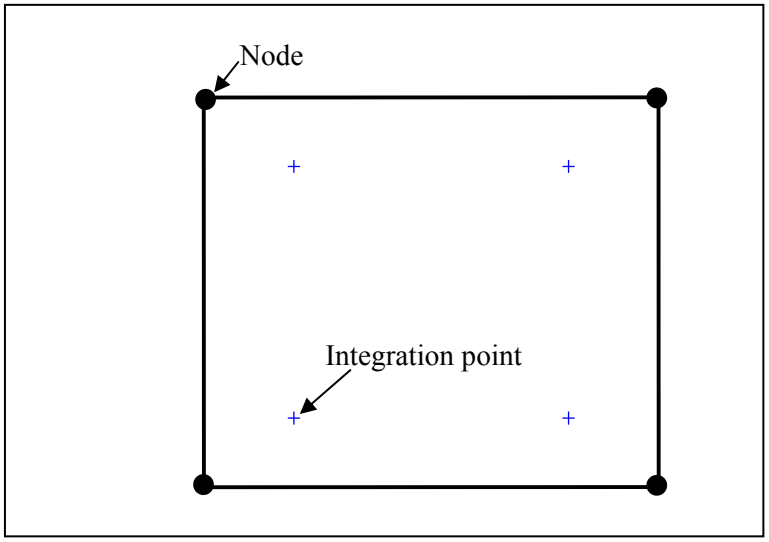

Figure 3.12 - Quadrilateral element of first order with full integration used in the research

3.9 Concluding remarks

The constitutive crack model adopted for the smeared crack analysis of concrete structures in this research has been presented. The crack initiation criterion and direction were described first. An enhanced mode I and II strain-softening strategy has been developed for this research. The conditions for subsequent new crack(s) to occur after the initial cracking have been established. Fixed or rotating cracks, a definition of crack closing and reopening, the crack mechanism for unloading and reloading, etc. have also been described. A bilinear mode I strain-softening formula has been given. The crack characteristic length h_c and the element type selected for this research have been defined.

The constitutive crack model proposed in this chapter will be fully implemented in an FE program in Chapter IV.